Polymer Chemistry

ROYAL SOCIETY OF CHEMISTRY

PAPER

View Article Online
View Journal

Open Access Article. Published on 16 January 2026. Downloaded on 1/17/2026 10:00:18 AM.
This article is licensed under a Creative Commons Attribution-NonCommercial 3.0 Unported Licence.

Check for updates

Cite this: DOI: 10.1039/d5py01139f

Uncovering a radical-mediated mechanism in the Kumada catalyst transfer polymerization of glycolated polythiophenes

Abdulrahman Bakry,[a,c] Preeti Yadav,[a] Wissem Khelifi,[a] Julia Khusnutdinova[b] and Christine Luscombe *[a]

Received 1st December 2025,
Accepted 31st December 2025

DOI: 10.1039/d5py01139f

rsc.li/polymers

Glycolated polythiophenes are of great interest for their use as organic mixed ionic-electronic conductors (OMIECs). In this study, we elucidate the polymerization mechanism for the synthesis of poly(3-((2-(2-methoxyethoxy)ethoxy)methyl)thiophene) (P3MEEMT) using Kumada catalyst transfer polymerization (KCTP). While the use of i-PrMgCl·LiCl (turbo-Grignard) for monomer activation enabled rapid polymerization within 10 min at room temperature, this resulted in lower than expected number-average molecular weight (M_n). We propose that the polymerization proceeds *via* a radical-mediated pathway, a mechanism not observed for poly(3-hexylthiophene) (P3HT). This was demonstrated by the complete inhibition of the reaction by the radical scavenger TEMPO and the detection of radical species by EPR spectroscopy using DMPO as a spin trap. By introducing $MgCl_2$ after Grignard metathesis, a controlled polymerization was afforded with M_n proportional to the catalyst loading. This work establishes that KCTP of glycolated thiophenes proceeds *via* a radical-assisted pathway and provides a strategy to control the polymer molecular weight. These findings establish a new principle for controlling polymerizations, where the monomer's physical aggregation state is the key factor in enabling a productive, radical-mediated pathway.

1. Introduction

Conjugated polymers are of interest in various scientific and commercial applications, as they are mechanically flexible, solution-processable, and have facile molecular design and synthetic strategies that can be used to tune both their optical and electronic properties.[1] Conjugated polymers have found applications in organic solar cells, sensing, and flexible electronic devices such as circuits and transistors due to their semiconducting properties,[2,3] solution processability,[4,5] flexibility,[6] large absorption,[7] adjusted band-gap,[8,9] low cytotoxicity,[10,11] ease of chemical modification and surface functionalization,[12] and their low-cost device fabrication methods.[4,6] Life science research innovation, particularly in medical diagnosis and health monitoring, has recently surged due to the integration of biological systems with electronic systems.[13] Organic electrochemical transistors (OECTs) have emerged as a significant technology in bioelectronics due to their high ability to convert biochemical signals into electrical ones,[14] allowing applications in various fields, including compact sensors, neuromorphic computing, and neural interfacing.[15] OECTs utilize electrochemical gating through an electrolyte to facilitate ion movement and generate electrical signals from the ionic ones.[16] This necessitates channel materials possessing mixed conduction properties of ionic and electronic species,[17–19] requiring a balance of carrier mobility and ion transport for optimal device performance. Conjugated polymers with ethylene glycol side chains have garnered attention as organic semiconductors due to their performance in OECT applications, offering synthetic flexibility, enhanced capacitance, and biocompatibility.[20–22] Various molecular design strategies, including mixed alkyl ethylene glycol chains,[23–26] altering chain lengths,[27,28] and modifying the backbone,[29–31] have been explored to improve the performance of these polymers. Despite significant progress, a controlled polymerization to synthesize these polymers remains elusive. Traditional metal-catalyzed polycondensation reactions are primarily used in the synthesis of conjugated polymers, which lack precise control over polymer characteristics such as regioregularity (RR) and number-average molecular weight (M_n), leading to polymers with large dispersities ($Đ$).[32–38] Recently,

[a]Pi-Conjugated Polymers Unit, Okinawa Institute of Science and Technology Graduate University, Kunigami-gun, Okinawa 904-0495, Japan. E-mail: christine.luscombe@oist.jp
[b]Coordination Chemistry and Catalysis Unit, Okinawa Institute of Science and Technology Graduate University, 1919-1 Tancha, Onna-son, Okinawa 904-0495, Japan
[c]Faculty of Science, Chemistry Department, Kafrelsheikh University, El Giesh Street, Kafrelsheikh 33516, Egypt

Open Access Article. Published on 16 January 2026. Downloaded on 1/17/2026 10:00:18 AM.
This article is licensed under a Creative Commons Attribution-NonCommercial 3.0 Unported Licence.

there has been a growing interest in cross-coupling polymerization employing a chain mechanism, which often relies on Kumada and Suzuki cross-coupling reactions catalyzed by nickel or palladium complexes.[38–42] In particular, Kumada catalyst transfer polymerization (KCTP), commonly used for the synthesis of polythiophenes, which starts with Grignard metathesis to activate a dihalomonomer followed by intramolecular catalyst transfer during polymerization, facilitates chain growth with living characteristics.[43–46]

Poly(3-((2-(2-methoxyethoxy)ethoxy)methyl)-thiophene) (P3MEEMT), with ethylene glycol-based side chains, has been widely studied as an organic mixed ionic–electronic conductor (OMIEC).[47–51] It is usually prepared by KCTP of the dihalomonomer using a nickel catalyst, but the M_n values are often low and not reaching the expected values.[52] In our previous study, the M_n trends were surprising, seemingly showing a decreasing M_n with increased reaction time with a maximum M_n obtained within 1 min of the polymerization.[53] Other previous synthetic strategies for P3MEEMT have primarily relied on lithiation or standard Grignard metathesis, achieving varying degrees of control. Early work by McCullough *et al.* used lithium diisopropylamide (LDA) followed by transmetalation with $MgBr_2$ and polymerization with Ni(dppp)Cl_2. While this method yielded highly regioregular polymers (99% HT couplings) with high molecular weights ($M_W \approx 71\,000$ g mol^{-1}), the reaction was sluggish (36 hours) and suffered from a broad dispersity ($Đ = 2$).[54] Subsequent studies investigated the influence of the catalyst ligand and monomer activation. Adachi *et al.* reported that the polymerization of the iodo-monomer, 2-bromo-5-iodo-3-[2-(2-methoxyethoxy)ethoxy]methylthiophene, using standard i-PrMgCl and Ni(dppe)Cl_2 at 0 °C yielded polymers with narrow dispersities (1.11–1.15).[55] As described later in the paper, this stands in contrast to our findings using turbo-Grignard (i-PrMgCl·LiCl). In our study, the activation of the iodo-monomer with turbo-Grignard resulted in no polymerization. Further developments in this space include the synthesis of block copolymers using 2-bromo-5-chloromagnesio-3-hexylthiophene. This work confirmed that Ni(dppe)Cl_2 provided improved control and narrower dispersities than Ni(dppp)Cl_2 for these systems.[56]

These counterintuitive and mixed results led us to investigate the mechanism of the polymerization further, focusing on why monomer conversion was low and what was causing the unexpectedly large M_n at the beginning of the polymerization. We hypothesized that 4 factors potentially drove the uncontrolled process: 1. undesirable regioisomer formation during Grignard metathesis potentially affecting monomer conversion;[57] 2. side chain oxygen coordination to Mg and perhaps to Ni;[58] 3. aggregation resulting from the Schlenk equilibrium;[59] 4. formation of radical species also as a result of the Schlenk equilibrium.[60]

Here, we report an investigation into this mechanism (Fig. 1a) and the subsequent optimization that successfully achieved a controlled polymerization (Fig. 1b). Our investigation revealed that monomer activation produces two regioisomers, which both react during the polymerization. The polymerization was completely quenched when a radical scavenger (2,2,6,6-tetramethylpiperidin-1-oxyl (TEMPO)) was added to the polymerization before catalyst addition, indicating the possibility of a radical-mediated reaction. This possibility was confirmed by reacting the activated monomer species with benzoquinone (BQ) and identifying the products by LC-MS. The radical character of this reaction is also evident in the EPR analysis of the activated monomer. This collective evidence points to a complex mechanism, distinct from standard KCTP, which we sought to understand and control.

1.1 Polymerization under standard conditions

A general polymerization procedure is shown in Fig. 2a. Monomer 2,5-dibromo-3-((2-(2-methoxyethoxy)ethoxy)methyl) thiophene (Br-3MEEMT-Br) was synthesized according to a literature procedure.[53] After Grignard metathesis, the product ratio was analyzed by ^{1}H NMR (Fig. 2b) using 1,3,5-trimethoxybenzene (TMB) as an internal standard. This analysis revealed a poor regioselectivity that disfavored the desirable product. The more hindered regioisomer (B) (from 2-position activation) was the major product (65%), while the less hindered, more desirable regioisomer (A) (from 5-position activation) was the minor product. This is in contrast to P3HT synthesis where it has been reported that the Grignard metathesis of 2,5-dibromo-3-hexylthiophene (Br-3HT-Br) results in two metalated regiochemical isomers where the major product (85%) is activated in the 5-position.[61] Subsequent polymerization using [1,2-bis(diphenylphosphino)ethane] dichloronickel(II) (Ni(dppe)Cl_2) in 1 mol% was performed to investigate the polymerization kinetics of P3MEEMT and examine the conversion of both regioisomers. Aliquots were taken at 1, 2, 4, 6, 8, and 10 min, and ^{1}H NMR was used to look at the monomer conversion. The data for the different time points are summarized in Table 1, entry 1, Fig. 2c, with all ^{1}H NMR spectra shown in Fig. S1–S6.

The ^{1}H NMR spectrum taken for the aliquot at 10 min (Fig. S6 and Fig. 2c), showed that a total monomer conversion of 44% was reached, where regioisomers A and B were incorporated in a 1 : 1.2 ratio. Given that the regioisomers A and B were in a 1 : 1.9 ratio at $t = 0$ min, this indicates that regioisomer A reacts faster than B as reflected in the ln $[M]_0/[M]$ *vs.* monomer conversion plot (Fig. 2e). As a result, despite regioisomer A being less abundant after Grignard metathesis, it is incorporated almost as much as regioisomer B in the final polymer. This is likely due to lower steric hinderance of regioisomer A. The reactivity also contrasts with what is observed during P3HT synthesis where the more sterically hindered monomer is not incorporated into the final polymer. These results indicate that the mix of regioisomers obtained is not the sole reason for the low monomer conversion and lack of control.

The M_n *vs.* monomer conversion (Fig. 2d) shows interesting trends as before. After 1 min (26% conversion), an M_n of 26 500 g mol^{-1} is achieved, after which the M_n drops, reaching a value of 8800 g mol^{-1} after 10 minutes. This indicates that a small population of monomer polymerizes rapidly initially.

Open Access Article. Published on 16 January 2026. Downloaded on 1/17/2026 10:00:18 AM.
This article is licensed under a Creative Commons Attribution-NonCommercial 3.0 Unported Licence.

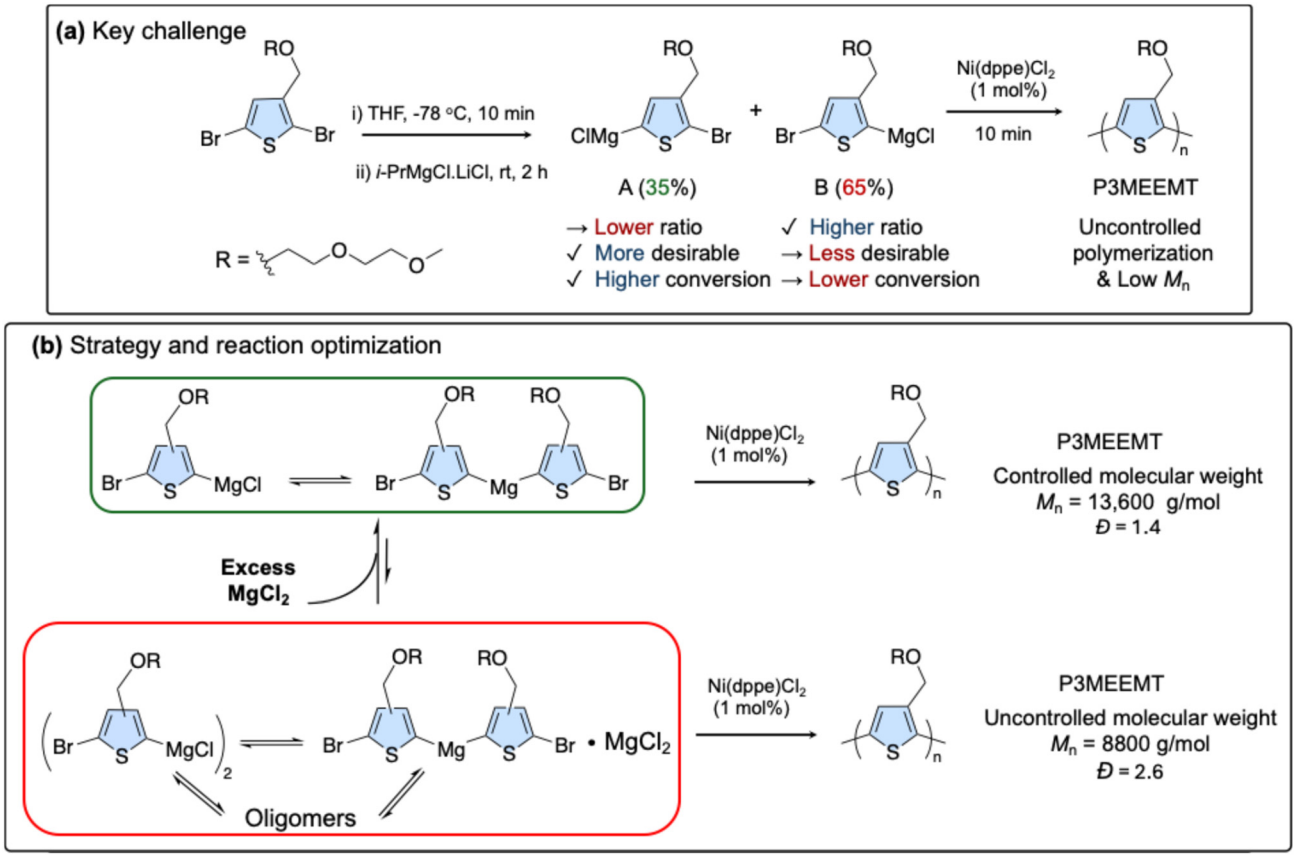

Fig. 1 Kumada catalyst-transfer polymerization (KCTP) of glycolated polythiophenes. (a) Challenges identified in previous studies and (b) the present strategy for optimizing the reaction to control molecular weight.

Given a monomer to catalyst ratio of 100 : 1, an M_n value of 21 000 g mol^{-1} was expected for complete conversion of both regioisomers and thus 9200 g mol^{-1} at 44% conversion.

1.2 Removing the regioisomer issue and indications of a radical-mediated pathway

Since both regioisomers are active towards polymerization, with greater reactivity realized in the less hindered one (*i.e.*, regioisomer A), we aimed to produce only one activated regioisomer from the Grignard metathesis at the 5-position. 2-Bromo-5-iodo-3-((2-(2-methoxyethoxy)ethoxy)methyl)thiophene (I-3MEEMT-Br) was synthesized following the procedure illustrated in Scheme 1, and the structure was determined using ^{1}H NMR and ^{13}C NMR (Fig. S7–S14). After Grignard activation of the monomer using 1 eq. of i-PrMgCl·LiCl, regioisomer A was obtained in 95% and the regioisomer B ratio was only 5% (Scheme 1, Fig. S15). Unexpectedly, upon addition of Ni(dppe)Cl$_2$, no polymerization was observed even after 60 minutes. We hypothesized that the reason for the polymerization failure was due to radical quenching by isopropyl iodide, a side-product during Grignard metathesis.[62,63]

To investigate the possibility of radical involvement in the reaction, TEMPO was added as a radical scavenger in a 1 : 1 ratio to the Grignard-activated Br-3MEEMT-Br monomer before adding the catalyst. This completely stopped the polymerization process without any noticeable conversion of both regioisomers (Table 1 (entry 2) and Fig. S16). It is worth noting that the polymerization still continues when synthesizing P3HT using the same conditions (Fig. S17). This suggests that the glycolated side chain of Br-3MEEMT-Br influences the radical character of the reaction. EPR analysis was conducted to detect the radical during both the Grignard metathesis and polymerization processes, comparing P3MEEMT and P3HT syntheses. Addition of DMPO, used as a spin trap at a 1 : 1 ratio to the turbo-Grignard reagent, produced a well-resolved 6-line EPR signal with hyperfine splitting constants of $a(^{14}\mathrm{N})$ = 1.39 mT and $a(^{1}\mathrm{H})$ = 1.96 mT during the Grignard metathesis of Br-3MEEMT-Br, as shown in Fig. 3. This matches previously reported hyperfine splitting parameters for the phenyl radical adduct of DMPO.[60] Conversely, no signal was detected in the case of 3HT. After the addition of Ni(dppe)Cl$_2$, the radical character in either polymerization could not be detected using DMPO as a spin trap at a 1 : 1 ratio with the catalyst after 10 minutes, even with a higher loading (20 mol%) of DMPO relative to the catalyst. Additionally, no EPR signal was observed in either the Grignard metathesis or polymerization when toluene replaced THF as the solvent, highlighting the solvent's influence on radical formation in Br-3MEEMT-Br.

Open Access Article. Published on 16 January 2026. Downloaded on 1/17/2026 10:00:18 AM.
This article is licensed under a Creative Commons Attribution-NonCommercial 3.0 Unported Licence.

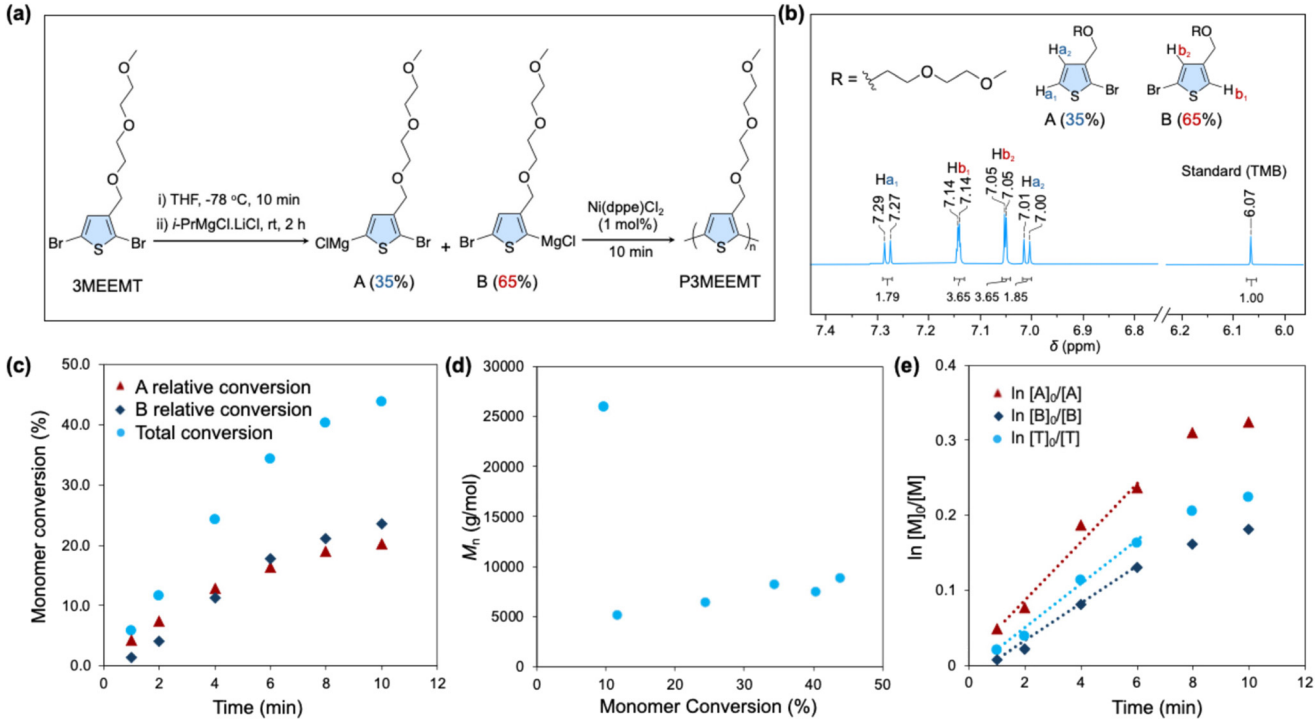

Fig. 2 (a) Grignard metathesis and polymerization of 3MEEMT. (b) ^{1}H NMR analysis in CD_2Cl_2 of the Grignard metathesis process of 3MEEMT. (c) Monomer conversion *vs.* time, (d) M_n *vs.* monomer conversion, and (e) ln([M]$_0$/[M]) *vs.* time under normal conditions.

Table 1 Monomer conversion and polymer characteristics under different reaction conditions

	Monomer conversion (%)	(A) relative conversion (%)	(B) relative conversion (%)	M_n (g mol^{-1})	RR	$Đ$
i-PrMgCl·LiCl	44	20	24	8800	85	2.6
i-PrMgCl·LiCl (TEMPO)	0	0	0	0	0	0
i-PrMgCl·LiCl (dark)	53	23	30	9200	88	2.8
i-PrMgCl·LiCl ($MgCl_2$)	73	21	52	**13 600**	84	1.4
i-PrMgCl·LiCl (DIPEA)	24	13	11	6300	83	2.8

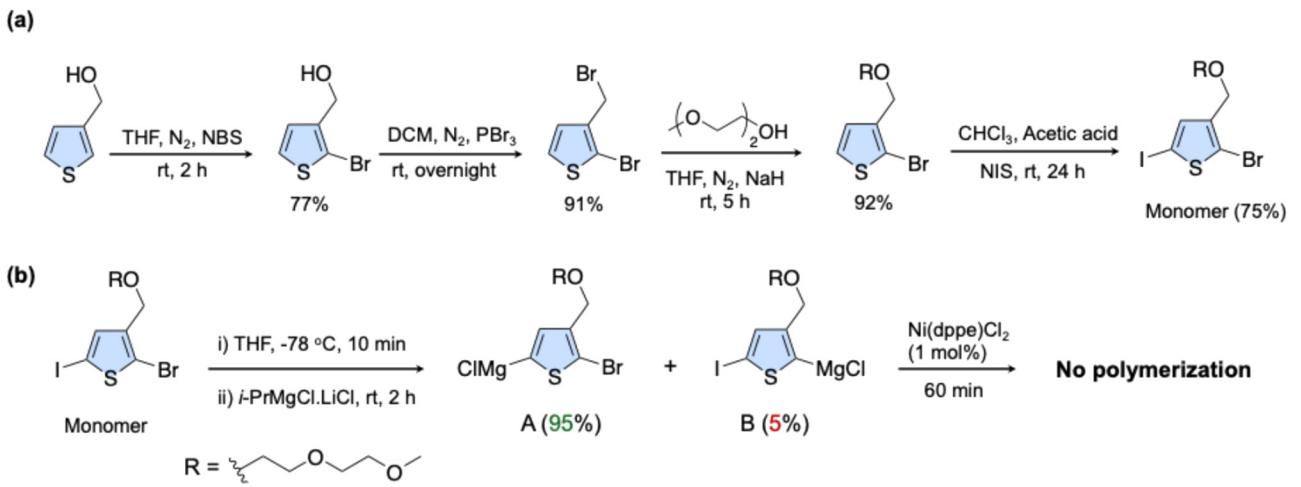

Scheme 1 (a) Synthesis, and (b) Grignard metathesis followed by polymerization of 2-bromo-5-iodo-3-((2-(2-methoxyethoxy)ethoxy)methyl) thiophene.

Open Access Article. Published on 16 January 2026. Downloaded on 1/17/2026 10:00:18 AM.
This article is licensed under a Creative Commons Attribution-NonCommercial 3.0 Unported Licence.

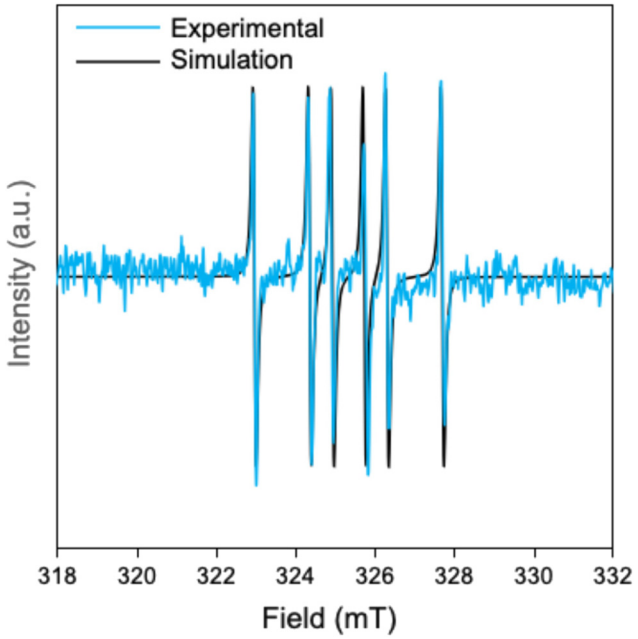

Fig. 3 EPR spectrum of Grignard-metathesized Br-3MEEMT-Br quenched with DMPO in THF. Experimental (blue) and simulated (black) EPR spectra. Simulation parameters: A_N = 1.39 mT, A_H = 1.96 mT, g = 2.007. Microwave frequency: 9137.6 MHz; recorded at RT.

These EPR results suggest the presence of aryl radicals after Grignard metathesis of the glycolated monomer in THF. The results also indicate that the glycolated side chain and solvent affect radical formation during the Grignard metathesis step. While the presence of radicals could not be confirmed at the end of the polymerization, this could be because the radical is short-lived or because the growing chain-end does not have radical character. The radical species formation is not photoinitiated,[64] as the polymerization under dark conditions behaves similarly to that under normal conditions. In dark polymerization, no significant change in the conversion ratios was observed (Table 1 (entry 3), Fig. S18–24) compared to normal conditions.

The presence of radical species in the Grignard metathesis was further examined by following a procedure in the literature, in which diaryl/dialkyl Grignards (R_2Mg) have been reported to facilitate single electron transfer (SET) more so than aryl/alkyl Grignards (RMgCl).[57] This gives rise to different products being observed when BQ is added to the Grignard mixture (Scheme 2). Specifically, R_2Mg is expected to give rise to the homocoupled product R_2. We quenched both activated monomers of Br-3MEEMT-Br and Br-3HT-Br with BQ, and analysed the resulting products *via* LC-MS. LC-MS showed peaks at 319, 427, and 613 *m*/*z* corresponding to the sodium salts of Br-3MEEMT-H, BQH-3MEEMTBr and Br-(3MEEMT)$_2$-Br, respectively (Fig. 4). The presence of the homocoupled product, Br-(3MEEMT)$_2$-Br, confirms that SET had occurred in our reaction mixture (Fig. 4c) supporting the presence of R_2Mg. In contrast, for Br-3HT-Br, products that would indicate SET were not observed.

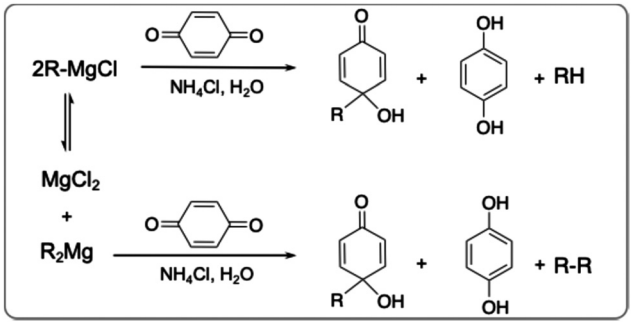

Scheme 2 Reaction of the aryl/alkyl Grignard *vs.* diaryl/dialkyl Grignard with BQ and the expected products.

1.3 The side chain's role in initiating the radical pathway

Grignard reagents are complex, coordinated species, not simple RMgX molecules as they are often depicted to be. They exist in a dynamic Schlenk equilibrium, which generates diarylmagnesium species (Ar_2Mg) and magnesium dihalides.[65] It has also been established that this equilibrium can be shifted by coordinating additives.[66] Ethers, such as dioxane, dimethoxyethane (DME), and other ethylene glycol derivatives (PEG250, or $Me(OCH_2CH_2)_4OMe$), have been shown to promote the formation of these diarylmagnesium species, often leading to enhanced reactivity (Fig. 5a). Based on this, we hypothesize that the ether oxygens on the 3MEEMT side chains act as coordinating agents. We postulate that this coordination shifts the Schlenk equilibrium towards the diarylmagneisum species (Fig. 5b), facilitating the SET pathway.

1.4 Optimization and achievement of a controlled polymerization

In order to reduce the radical character in the reaction, we hypothesized that the addition of $MgCl_2$ would push the Schlenk equilibrium back to the aryl magnesiate species. With this in mind, polymerization was carried out by adding 1 eq. of $MgCl_2$ to the metathesized monomer. A significantly enhanced total monomer conversion 74% was achieved of which 21% corresponded to regioisomer A and 53% corresponded to regioisomer B (Table 1 (entry 4), Fig. 6a, and S25–S35). A linear relationship was observed between the M_n values and monomer conversion (Fig. 6b and Fig. S48) indicative of a more controlled polymerization. While M_n *vs.* conversion does remain linear till high conversion (Fig. S48), the GPC traces suggest that after 10 minutes, some chains are beginning to terminate and only some chains continue to grow, as shown by the constant peak retention volume and widening dispersity (Table S1).

Comparing the polymerization kinetics under standard conditions to those with added $MgCl_2$, total monomer conversion increased significantly from 44% to 74%. A notable change was observed in the reactivity of regioisomer B. While it reacts more slowly than regioisomer A under standard conditions, the addition of $MgCl_2$ allows regioisomer B to react as fast as regioisomer A. This is illustrated in the ln $[M]_0/[M]$ *vs.* monomer conversion plot (Fig. 2e and 6c). We attribute this enhanced reactivity

Open Access Article. Published on 16 January 2026. Downloaded on 1/17/2026 10:00:18 AM.
This article is licensed under a Creative Commons Attribution-NonCommercial 3.0 Unported Licence.

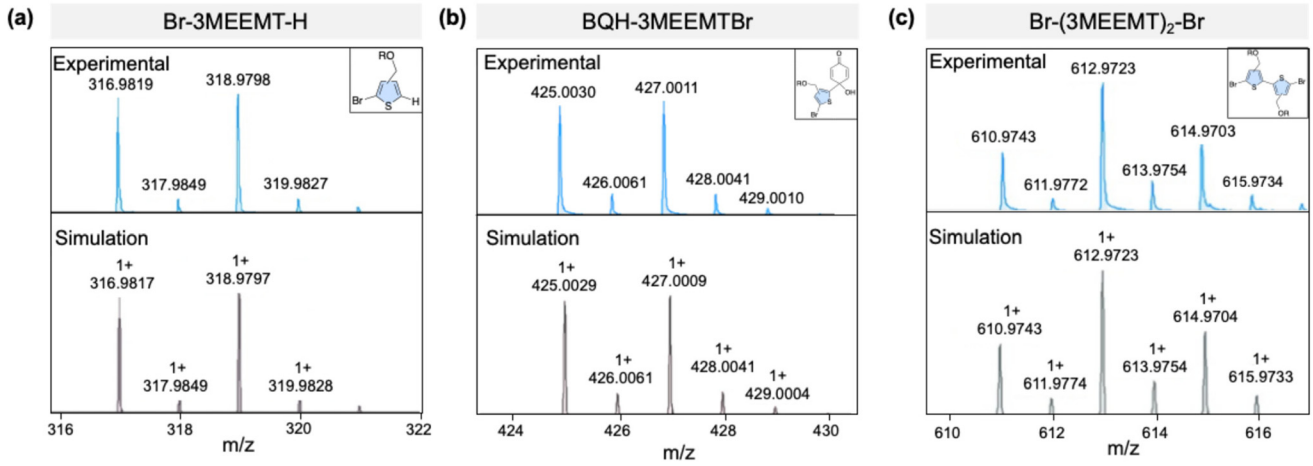

Fig. 4 (a) LC-MS spectra of the sodium salt of crude product of the Grignard-metathesized Br-3MEEMT-Br reaction with BQ in THF. (a) Br-3MEEMT-H, (b) BQH-3MEEMTBr, and (c) Br-(3MEEMT)$_2$-Br.

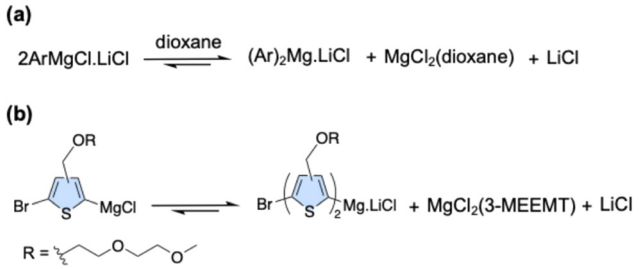

Fig. 5 (a) Dioxane shifts the equilibrium towards the dialkyl/diaryl magnesium species. (b) Hypothesized equilibrium of Br-3MEEMT-MgCl with coordination of the side chain pushing the equilibrium towards the diaryl magnesium species.

to the role of $MgCl_2$ as a disaggregating agent, which reduces the formation of inactive species and effectively diminishes the steric hindrance surrounding regioisomer B.

Despite the presence of both regioisomers in the final polymer, the regioregularity remained consistently around 85% across different conditions (Table 1). This regioregularity was determined by integrating the methylene peak at 4.65 ppm (Fig. S6, S23, S35, and S39). The high degree of regioregularity, given the simultaneous and differing incorporation of both isomers, suggests that the reaction proceeds *via* a block-like or gradient polymerization rather than a random incorporation of monomers.

Interestingly, no polymerization was observed when 1 eq. of TEMPO was added to the monomer after $MgCl_2$ addition indicating that the radical species were still present (Fig. S36). This implies that the addition of $MgCl_2$ did not necessarily affect the traditional Schlenk equilibrium and affect the ratio between arylmagnesiate *vs.* diarylmagnesiate. The Schlenk equilibrium is now understood to be more complex, involving arylmagnesiate, diarylmagnesiate, aggregations, and oligomeric species,[53] so we believe that the reaction was facilitated by converting these aggregated/oligomeric species back to the monomeric species.

The hypothesis that the polymerization is sensitive to the monomer's aggregation state was probed using reactions with

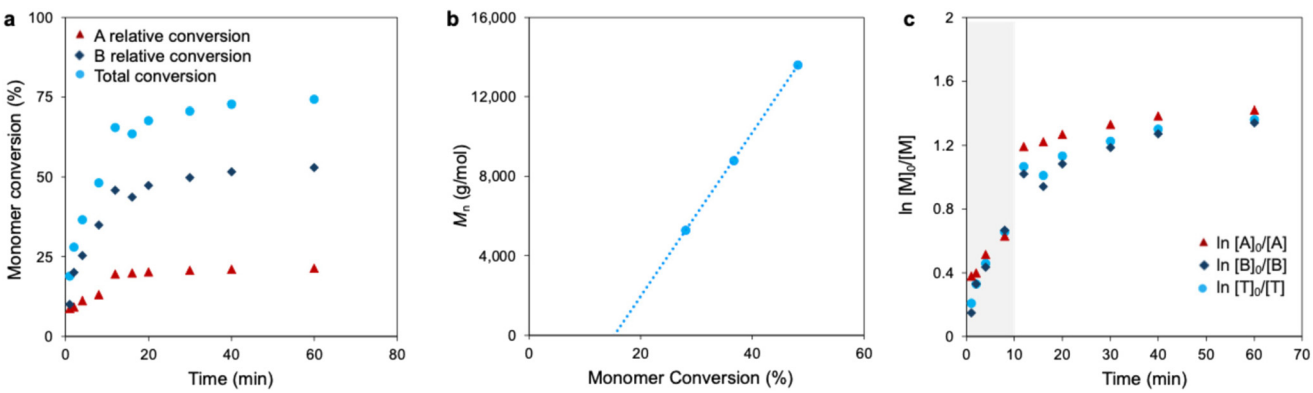

Fig. 6 (a) Monomer conversion *vs.* time, (b) M_n *vs.* monomer conversion, and (c) ln([M]$_0$/[M]) *vs.* time for polymerization conducted with $MgCl_2$ (1 eq.) after the Grignard metathesis process.

Open Access Article. Published on 16 January 2026. Downloaded on 1/17/2026 10:00:18 AM.
This article is licensed under a Creative Commons Attribution-NonCommercial 3.0 Unported Licence.

other coordinating and non-coordinating additives. The reaction was completely stopped with a strongly coordinating additive when dioxane (1 eq.) was added to the THF solution (Fig. S37). This suggests that the equilibrium was pushed toward an inactive, locked aggregated state. Crucially, the polymerization of 3HT, which is less sensitive to this aggregation, proceeded in dioxane (Fig. S38), highlighting the specific role of the 3MEEMT side chain. The sensitivity to coordination was further demonstrated by the addition of *N*,*N*-diisopropylethylamine (DIPEA) 1 eq. where reduced monomer conversion of 24% was observed (Table 1 (entry 5), Fig. S39 and S40). Similarly, *N*,*N*,*N*′,*N*′-tetramethylethylenediamine (TMEDA) 1 eq. reduced monomer conversion to 38% (Fig. S41 and S42). The addition of LiCl, which is often used to break up the aggregates in this reaction, was found to completely stop the polymerization suggesting that the lithium magnesiate is too stable for this polymerization. Finally, the polymerization was completely stopped when using a non-coordinating solvent toluene (Fig. S43), suggesting that the polymerization is extremely sensitive to Grignard speciation. These results reveal that the polymerization exists in a very delicate and complex equilibrium. The polar side chain enables a rapid, radical-mediated pathway; however, the concurrent formation of inactive aggregates is a limiting factor.

The standard KCTP cycles through Ni(0) and Ni(II) oxidation states in the catalytic cycle. Although we could not observe the radical species during the polymerization, their presence in the activated monomer cannot preclude the change in mechanism that involves the Ni(I)/Ni(II)/Ni(III) relay[67] or a catalytic cycle that involves Ni(I) and Ni(III) oxidation states especially in the presence of coordinating solvent.[68] Future work will focus on elucidation of this mechanism.

2. Conclusions

In conclusion, we have demonstrated that the KCTP of 3MEEMT proceeds *via* a radical-mediated mechanism, a pathway not observed for P3HT. We found that the coordinating glycol side chain is responsible for both initiating this radical pathway and for promoting the formation of inactive aggregates. Under standard THF conditions, these aggregates act as a limiting factor, resulting in an uncontrolled polymerization with low M_n values. This sensitivity to aggregation was further highlighted by the reaction's failure in both non-coordinating toluene and strongly-coordinating dioxane, as well as the addition of LiCl. We discovered that this radical pathway could be modulated through the addition of $MgCl_2$. We hypothesize that $MgCl_2$ acts as a dis-aggregating agent, suppressing the inactive aggregates and enabling a more controlled polymerization. This work demonstrates that by managing the aggregation state of the monomer, we can achieve molecular weight control of this radical-mediated polymerization. It also expands the mechanistic scope of KCTP by identifying a hitherto unobserved radical pathway.

Author contributions

A. B.: investigation, methodology, validation, writing, and data curation. P. Y.: assistance with GPC, review & editing. W. K.: assistance with GPC analysis, review & editing. J. K.: assistance with the EPR analysis. C. L.: methodology, conceptualization, writing, review & editing, supervision, and funding acquisition.

Conflicts of interest

There are no conflicts to declare.

Data availability

The relevant data supporting this article have been included as part of the supplementary information (SI). Supplementary information: materials and methods, synthesis of I-3MEEMT-Br, KCTP polymerizations, NMR analyses, and GPC measurements. See DOI: https://doi.org/10.1039/d5py01139f.

Acknowledgements

This work was supported by funding from the Okinawa Institute of Science and Technology (OIST) and JSPS KAKENHI Grants No. 24K08518. We thank Dr Michael Roy (Instrumental Analysis Section, OIST Core Facility) for the help during mass spectrometry measurements. Additionally, we appreciate the support from Dr Fathy Hassan (π-Conjugated Polymers Unit, OIST) for valuable discussions. We thank the Instrumental Analysis Section at OIST for technical support.

References

1 S. Kang, T. W. Yoon, G. Y. Kim and B. Kang, *ACS Appl. Nano Mater.*, 2022, **5**(12), 17436–17460.
2 T. F. Abelha, T. W. Phillips, J. H. Bannock, A. M. Nightingale, C. A. Dreiss, E. Kemal, L. Urbano, J. C. deMello, M. Green and L. A. Dailey, *Nanoscale*, 2017, **9**(5), 2009–2019.
3 A. Ghosh, B. Jana, S. Chakraborty, S. Maiti, B. Jana, H. N. Ghosh and A. Patra, *J. Phys. Chem. C*, 2017, **121**(38), 21062–21072.
4 S. H. Yu, H. G. Song, J. Cho, S.-K. Kwon, Y.-H. Kim and D. S. Chung, *Chem. Mater.*, 2018, **30**(14), 4808–4815.
5 W. Dong, Z. Ma, Q. Duan and T. Fei, *Dyes Pigm.*, 2018, **159**, 128–134.
6 L. Parrenin, C. Brochon, G. Hadziioannou and E. Cloutet, *Macromol. Rapid Commun.*, 2015, **36**(20), 1816–1821.
7 C. Negele, J. Haase, A. Leitenstorfer and S. Mecking, *ACS Macro Lett.*, 2012, **1**(11), 1343–1346.
8 N. Anwar, A. Rix, W. Lederle and A. J. Kuehne, *Chem. Commun.*, 2015, **51**(45), 9358–9361.

Open Access Article. Published on 16 January 2026. Downloaded on 1/17/2026 10:00:18 AM.
This article is licensed under a Creative Commons Attribution-NonCommercial 3.0 Unported Licence.

9 J. M. Behrendt, J. A. E. Guzman, L. Purdie, H. Willcock, J. J. Morrison, A. B. Foster, R. K. O'Reilly, M. C. McCairn and M. L. Turner, *React. Funct. Polym.*, 2016, **107**, 69–77.
10 J. Nette, P. D. Howes and A. J. deMello, *Adv. Mater. Technol.*, 2020, **5**(7), 2000060.
11 J. Pecher, J. Huber, M. Winterhalder, A. Zumbusch and S. Mecking, *Biomacromolecules*, 2010, **11**(10), 2776–2780.
12 B. Jana, S. Bhattacharyya and A. Patra, *Bull. Mater. Sci.*, 2018, **41**(5), 122–131.
13 Y. Fang, L. Meng, A. Prominski, E. N. Schaumann, M. Seebald and B. Tian, *Chem. Soc. Rev.*, 2020, **49**, 7978–8035.
14 A. Marks, S. Griggs, N. Gasparini and M. Moser, *Adv. Mater. Interfaces*, 2022, **9**, 2102039.
15 A. Melianas, T. J. Quill, G. LeCroy, Y. Tuchman, H. V. Loo, S. T. Keene, A. Giovannitti, H. R. Lee, I. P. Maria, I. McCulloch and A. Salleo, *Sci. Adv.*, 2020, **6**, eabb2958.
16 J. Rivnay, S. Inal, A. Salleo, R. M. Owens, M. Berggren and G. G. Malliaras, *Nat. Rev. Mater.*, 2018, **3**, 1–14.
17 X. Wu, Q. Liu, A. Surendran, S. E. Bottle, P. Sonar and W. L. Leong, *Adv. Electron. Mater.*, 2021, **7**, 2000701.
18 S. Inal, J. Rivnay, P. Leleux, M. Ferro, M. Ramuz, J. C. Brendel, M. M. Schmidt, M. Thelakkat and G. G. Malliaras, *Adv. Mater.*, 2014, **26**, 7450–7455.
19 M. Moser, J. F. Ponder Jr, A. Wadsworth, A. Giovannitti and I. McCulloch, *Adv. Funct. Mater.*, 2019, **29**, 1807033.
20 S. E. Chen, L. Q. Flagg, J. W. Onorato, L. J. Richter, J. Guo, C. K. Luscombe and D. S. Ginger, *J. Mater. Chem. A*, 2022, **10**, 10738–10749.
21 S. Inal, G. G. Malliaras and J. Rivnay, *Nat. Commun.*, 2017, **8**, 1767.
22 N. A. Kukhta, A. Marks and C. K. Luscombe, *Chem. Rev.*, 2021, **122**, 4325–4355.
23 P. Li and T. Lei, *J. Polym. Sci.*, 2022, **60**, 377–392.
24 R. Halaksa, J. H. Kim, K. J. Thorley, P. A. Gilhooly-Finn, H. Ahn, A. Savva, M.-H. Yoon and C. B. Nielsen, *Angew. Chem.*, 2023, **135**, e202304390.
25 E. Tan, J. Kim, K. Stewart, C. Pitsalidis, S. Kwon, N. Siemons, J. Kim, Y. Jiang, J. M. Frost and D. Pearce, *Adv. Mater.*, 2022, **34**, 2202574.
26 I. P. Maria, B. D. Paulsen, A. Savva, D. Ohayon, R. Wu, R. Hallani, A. Basu, W. Du, T. D. Anthopoulos and S. Inal, *Adv. Funct. Mater.*, 2021, **31**, 2008718.
27 B. T. DiTullio, L. R. Savagian, O. Bardagot, M. De Keersmaecker, A. M. Österholm, N. Banerji and J. R. Reynolds, *J. Am. Chem. Soc.*, 2022, **145**, 122–134.
28 P. Schmode, A. Savva, R. Kahl, D. Ohayon, F. Meichsner, O. Dolynchuk, T. Thurn-Albrecht, S. Inal and M. Thelakkat, *ACS Appl. Mater. Interfaces*, 2020, **12**, 13029–13039.
29 K. Feng, W. Shan, J. Wang, J. W. Lee, W. Yang, W. Wu, Y. Wang, J. B. Kim, X. Guo and H. Guo, *Adv. Mater.*, 2022, **34**, 2201340.
30 I. P. Maria, S. Griggs, R. B. Rashid, B. D. Paulsen, J. Surgailis, K. Thorley, V. N. Le, G. T. Harrison, C. Combe and R. Hallani, *Chem. Mater.*, 2022, **34**, 8593–8602.
31 J. Chen, S. Cong, L. Wang, Y. Wang, L. Lan, C. Chen, Y. Zhou, Z. Li, I. McCulloch and W. Yue, *Mater. Horiz.*, 2023, **10**, 607–618.
32 P. Schmode, D. Ohayon, P. M. Reichstein, A. Savva, S. Inal and M. Thelakkat, *Chem. Mater.*, 2019, **31**, 5286–5295.
33 X. Guo and A. Facchetti, *Nat. Mater.*, 2020, **19**, 922–928.
34 H. Shirakawa, E. J. Louis, A. G. MacDiarmid, C. K. Chiang and A. J. Heeger, *J. Chem. Soc., Chem. Commun.*, 1977, 578–580.
35 S. C. Rasmussen, *ChemPlusChem*, 2020, **85**, 1412–1429.
36 A. R. Murad, A. Iraqi, S. B. Aziz, N. Abdullah and M. A. Brza, *Polymers*, 2020, **12**, 2627.
37 A. Yokoyama and T. Yokozawa, *Macromolecules*, 2007, **40**, 4093–4101.
38 S. B. Mdluli, M. E. Ramoroka, S. T. Yussuf, K. D. Modibane, V. S. John-Denk and E. I. Iwuoha, *Polymers*, 2022, **14**, 716.
39 X. Guo and A. Facchetti, *Nat. Mater.*, 2020, **19**, 922–928.
40 H. Murakami, K. Kobayashi, K. Suzuki, T. Yasuda, T. Kanbara and J. Kuwabara, *Macromolecules*, 2021, **54**, 11281–11288.
41 E. E. Sheina, J. Liu, M. C. Iovu, D. W. Laird and R. D. McCullough, *Macromolecules*, 2004, **37**, 3526–3528.
42 A. Yokoyama, R. Miyakoshi and T. Yokozawa, *Macromolecules*, 2004, **37**, 1169–1171.
43 M. V. Bautista, A. J. Varni, J. Ayuso-Carrillo, C.-H. Tsai and K. J. T. Noonan, *ACS Macro Lett.*, 2020, **9**, 1357–1362.
44 J. Lee, H. Kim, H. Park, T. Kim, S.-H. Hwang, D. Seo, T. D. Chung and T.-L. Choi, *J. Am. Chem. Soc.*, 2021, **143**, 11180–11190.
45 S. Cheng, R. Zhao and D. S. Seferos, *Acc. Chem. Res.*, 2021, **54**, 4203–4214.
46 Y. He and C. K. Luscombe, *Polym. Chem.*, 2024, **15**, 2598–2605.
47 S. Inal, G. G. Malliaras and J. Rivnay, *Nat. Commun.*, 2017, **8**, 1767.
48 L. Q. Flagg, C. G. Bischak, J. W. Onorato, R. B. Rashid, C. K. Luscombe and D. S. Ginger, *J. Am. Chem. Soc.*, 2019, **141**, 4345–4354.
49 R. S. Loewe, S. M. Khersonsky and R. D. McCullough, *Adv. Mater.*, 1999, **11**, 250–253.
50 S. E. Chen, L. Q. Flagg, J. W. Onorato, L. J. Richter, J. Guo, C. K. Luscombe and D. S. Ginger, *J. Mater. Chem. A*, 2022, **10**, 10738–10749.
51 J. W. Onorato, Z. Wang, Y. Sun, C. Nowak, L. Q. Flagg, R. Li, B. X. Dong, L. J. Richter, F. A. Escobedo, P. F. Nealey, S. N. Patel and C. K. Luscombe, *J. Mater. Chem. A*, 2021, **9**, 21410–21423.
52 B. X. Dong, C. Nowak, J. W. Onorato, J. Strzalka, F. A. Escobedo, C. K. Luscombe, P. F. Neale and S. N. Patel, *Chem. Mater.*, 2019, **31**, 1418–1429.
53 R. D. McCullough and S. P. Williams, *J. Am. Chem. Soc.*, 1993, **115**, 11608–11609.
54 I. Adachi, R. Miyakoshi, A. Yokoyama and T. Yokozawa, *Macromolecules*, 2006, **39**, 7793–7795.
55 T. Yokozawa, I. Adachi, R. Miyakoshi and A. Yokoyama, *High Perform. Polym.*, 2007, **19**, 684–699.
56 A. Bakry, P. Yadav, S. Y. E. Chen and C. K. Luscombe, *Faraday Discuss.*, 2024, **250**, 74–82.

Open Access Article. Published on 16 January 2026. Downloaded on 1/17/2026 10:00:18 AM.
This article is licensed under a Creative Commons Attribution-NonCommercial 3.0 Unported Licence.

57 G. Koeckelberghs, M. Vangheluwe, K. V. Doorsselaere, E. Robijns, A. Persoons and T. Verbiest, *Macromol. Rapid Commun.*, 2006, **27**, 1920–1925.
58 N. Yoshikai, H. Matsuda and E. Nakamura, *J. Am. Chem. Soc.*, 2009, **131**, 9590–9599.
59 R. M. Peltzer, O. Eisenstein, J. Gauss and M. Cascella, *J. Phys. Chem. B*, 2017, **121**, 4226–4237.
60 T. Ramnial, S. A. Taylor, J. A. C. Clyburne and C. J. Walsby, *Chem. Commun.*, 2007, **20**, 2066–2068.
61 R. S. Loewe, P. C. Ewbank, J. Liu, L. Zhai and R. D. McCullough, *Macromolecules*, 2001, **34**, 4324–4333.
62 G. C. Fu, *ACS Cent. Sci.*, 2017, **3**, 692–700.
63 S. Mistry, R. Kumar, A. Lister and M. J. Gaunt, *Chem. Sci.*, 2022, **13**, 13241–13247.
64 E. F. Woods, A. J. Berl, L. P. Kantt, C. T. Eckdahl, M. R. Wasielewski, B. E. Haines and J. A. Kalow, *J. Am. Chem. Soc.*, 2021, **143**, 18755–18765.
65 W. Schlenk and W. Schlenk Jr., *Ber. Dtsch. Chem. Ges. B*, 1929, **62**, 920–924.
66 A. Krasovskiy, B. F. Straub and P. Knochel, *Angew. Chem., Int. Ed.*, 2006, **45**, 159–162.
67 H. Yin and G. C. Fu, *J. Am. Chem. Soc.*, 2019, **141**, 15433–15440.
68 L. Griego, J. B. Chae and L. M. Mirica, *Chem*, 2024, **10**, 867–881.